MODELAGEM MATEMÁTICA DA DINÂMICA DA ADSORÇÃO ISOTÉRMICA DE NÃO-EQUILÍBRIO DO DIÓXIDO DE CARBONO

MATHEMATICAL MODELING OF THE DYNAMICS OF NON-EQUILIBRIUM ISOTHERMAL ADSORPTION OF CARBON DIOXIDE

МАТЕМАТИЧЕСКОЕ МОДЕЛИРОВАНИЕ ДИНАМИКИ НЕРАВНОВЕСНОЙ ИЗОТЕРМИЧЕСКОЙ АДСОРБЦИИ УГЛЕКИСЛОГО ГАЗА

ASTAPOV, Alexey N.[1*]; KURBATOV, Alexey S.[2]; RABINSKIY, Lev N.[1]; TARASOVA, Anna N.[3]

[1] Moscow Aviation Institute (National Research University), Department of Advanced Materials and Technologies for Aerospace Application, 4 Volokolamskoe shosse, zip code 125993, Moscow – Russian Federation
(phone: ++74991584264)

[2] Moscow Aviation Institute (National Research University), Department of Mechanics of Nanostructured Materials and Systems, 4 Volokolamskoe shosse, zip code 125993, Moscow – Russian Federation
(phone: +74991582977)

[3] Moscow Aviation Institute (National Research University), Department of Engineering Graphics, 4 Volokolamskoe shosse, zip code 125993, Moscow – Russian Federation
(phone: +74991584551)

** Corresponding author*
e-mail: lexxa1985@inbox.ru

Received 25 June 2017; received in revised form 30 November 2018; accepted 02 December 2018

RESUMO

Um modelo matemático adequado da dinâmica de adsorção isotérmica de não-equilíbrio de dióxido de carbono no cartucho de absorção de uma instalação modelo para a regeneração da atmosfera de objetos autônomos (espaçonaves, navios e estações, submarinos, cápsulas, etc.) é proposto. Um algoritmo foi desenvolvido para solução numérica do problema usando a versão longitudinal do método de linhas, o método de continuação da solução com relação ao melhor parâmetro e as fórmulas implícitas de derivação multi-passo inversa com controle adaptativo da ordem das fórmulas e a magnitude da etapa de integração. Os cálculos paramétricos de adsorção de dióxido de carbono por um absorvente baseado em hidróxido de ferro são realizados em uma ampla gama de parâmetros determinantes: concentração de gás de entrada, taxa de filtração de gás, valores do coeficiente de adsorção cinética.

Palavras-chave: *adsorção isotérmica, transferência de massa, sistema de suporte à vida, modelagem matemática, fórmula de diferenciação inversa.*

ABSTRACT

An adequate mathematical model of the dynamics of the nonequilibrium isothermal adsorption of carbon dioxide in the absorption cartridge of the model installation for the regeneration of the atmosphere of autonomous objects (space vehicles, ships, and stations, submarines, capsules, etc.) is proposed. An algorithm for the numerical solution of the problem is developed using the longitudinal variant of the method of straight lines, the method of continuation of the solution with respect to the best parameter, and implicit multi-step rear differentiation formulas with adaptive control of the order of the formulas and the magnitude of the integration step. Parametric calculations of the adsorption of carbon dioxide by sorbent on the basis of iron hydroxide in a wide range of determining parameters were performed: the inlet gas concentration, the gas filtration rate, and the kinetic adsorption coefficient.

Keywords: *isothermal adsorption, mass transfer, life support system, mathematical modeling, backward differentiation formula.*

DOI: 10.52571/PTQ.SI1.2018.149_PeriodicoES.pdf

АННОТАЦИЯ

Предложена адекватная математическая модель динамики неравновесной изотермической адсорбции углекислого газа в поглотительном патроне модельной установки для регенерации атмосферы автономных объектов (космические аппараты, корабли и станции, подводные лодки, капсулы и т.п.). Разработан алгоритм численного решения задачи с использованием продольного варианта метода прямых, метода продолжения решения по наилучшему параметру и неявных многошаговых формул дифференцирования назад с адаптивным контролем порядка формул и величины шага интегрирования. Проведены параметрические расчеты адсорбции углекислого газа сорбентом на основе гидроксида железа в широком диапазоне определяющих параметров: входной концентрации газа, скорости фильтрации газа, значений кинетического коэффициента адсорбции.

Ключевые слова: *адсорбция изотермическая, массоперенос, система жизнеобеспечения, моделирование математическое, backward differentiation formula.*

INTRODUCTION

Nowadays, the task of developing new generations of technical systems that provide conditions for human life during its long stay in hermetically enclosed volumes (space vehicles, ships, and stations, submarines, capsules for various purposes, etc.) is becoming increasingly actual. The life support system for autonomous objects is usually constructed in a closed loop, based on the concentration of carbon dioxide from a stream taken directly from the habitat, followed by the recovery of oxygen from it through the Sabatier reaction (Budiman and Zuas, 2015). The results of a critical analysis of possible ways of extracting and concentrating carbon dioxide in air regeneration systems are presented in the work (Posternak *et al.*, 2012). It has been shown that the most effective and economically feasible methods are based on the use of cyclic adsorption processes, which in their essence are a complex system of mass exchange, thermal, hydromechanical and chemical processes (Keltsev, 1984; Shumyatsky, 2009; Rachinsky, 1964; Besedova *et al.*, 2004).

In the life support system, semi-automatic and automatic control modes are usually provided. In the latter case, the operator specifies the allowable partial pressure of CO_2 in the atmosphere of a closed object (for example, GOST R 50804-95, 1995), and in the computing device of the system an appropriate mode is chosen, realizing, as a rule, a rigidly defined algorithm for the functioning of a life support system with constant parameters. A very important and actual task is the creation of control systems that can adequately respond to the dynamic changes in the composition of the atmosphere, take into account the necessary switching in the states of the functioning of the system (for example, for various types of crew load – sleep, peace, work of medium intensity, hard work) provide the most comfortable conditions for life at any time intervals. This task is complex, and its solution is a complicated multi-stage process comprising the creation of full-scale experimental apparatus, development of an adequate mathematical model and algorithm engineering calculations, the implementation of the identification of the model parameters (Li *et al.*, 2017), the development of an algorithm of optimal control, creation of software and hardware complex control system automation, carrying out of verification procedures, validation, etc.

This work is a continuation of systematic studies of processes in absorbers of atmospheric purification systems of autonomous objects. In previous works (Tarasova, 2011; Rabinsky and Tarasova, 2011; Tarasova and Rabinsky, 2010; Kuznetsova and Tarasova, 2008; Rabinsky and Tarasova, 2009; Rabinsky and Tarasova, 2012; Tarasova, 2013), a detailed description of the main physical processes is presented and a closed system of equations is obtained that simulate in general the processes of heat and mass transfer in a layer of granular material that is filtering gas. The aim of this work is the development of a mathematical model, an algorithm for constructing a solution, and calculating the dynamics of the nonequilibrium isothermal adsorption of carbon dioxide in the absorption cartridge of the experimental setup for the regeneration of the atmosphere in a hermetically closed volume.

MATERIALS AND METHODS

2.1. Experimental installation for gas environment regeneration

The unit is designed to remove carbon dioxide and water vapor from the atmosphere of inhabited hermetically sealed volumes. It consists of two main blocks: the gas pre-drying unit and the carbon dioxide absorption unit.

In order to increase the efficiency of the regeneration of the atmosphere in hermetic objects and to reduce the loss of moisture, humid air containing carbon dioxide is taken from the environment and first passed through the drying cartridges of the first block. In this case, water vapor is absorbed by the granules of the sorbent material (for example, silica gel). In this case, only water vapor is absorbed, since H_2O molecules have a higher sorption potential than molecules of other air components. Studies of the processes taking place in the unit for preliminary drying of the gas of the installation are discussed in works (Tarasova, 2011; Rabinsky and Tarasova, 2011; Tarasova and Rabinsky, 2010; Kuznetsova and Tarasova, 2008).

Then, dried air with an increased CO_2 content passes through a layer of granular sorbent of the carbon dioxide absorption unit. As sorbents of CO_2, metal hydroxides – iron, nickel, zirconium, and also amino acids are widely used in the world (Posternak *et al*., 2012). *The sorption stage* continues until the CO_2 concentration at the outlet from the absorption cartridge exceeds the predetermined level (bypass starts). After that, the air supply to the unit stops, and a saturated or slightly overheated water vapor is passed through the sorbent layer. As a result of the heating of the layer, it exchanges with the flow of condensing vapor and the CO_2 molecules are displaced from the pores by water vapor possessing a higher sorption potential, there is an intensive liberation of carbon dioxide from the sorbent granules (at the *desorption stage*). Simultaneous flow of desorption processes in the anterior, more heated part of the layer and sorption in its less heated part, located downstream, causes the formation of a steep front of carbon dioxide concentration in the stream (Formalev *et al*., 2015). Therefore, the removal of desorbed CO_2 from the unit occurs by simply evacuating the gas displaced by the steam. The sorbent layer, purified from CO_2 in this way, contains a large amount of moisture and has a high temperature (~ 100 ° C). To complete the process of regeneration of the absorption cartridge and restore its initial sorption properties, it is necessary to cool the sorbent and reduce its moisture content. This is achieved by passing air through the mixture at a flow rate of ~ 20% of the nominal value (*drying stage*).

The present work is devoted to mathematical modeling of the processes taking place at the first of the three stages of cyclic operation of the carbon dioxide absorption block – the sorption stage. The adsorption scheme of the CO_2 absorption block, its geometric dimensions and the directions of the air flow are shown in Figure 1. The central beaker and the absorber walls are made of austenitic grade steel grade 12H18N10T, 1 mm thick. Outside, the unit is insulated. As a sorbent CO_2 in the present work, a granular absorber based on iron hydroxide having the following characteristics is used: bulk density ρ_b = 1.1 g/cm^3, grain size d = 2 mm, porosity ε = 0.4.

2.2. A mathematical model of the dynamics of nonequilibrium isothermal adsorption

The substantiation of the basic equations of adsorption dynamics and their analysis in general form are given in monographs (Keltsev, 1984; Shumyatsky, 2009; Rachinsky, 1964). Below we shall consider these equations in a simpler form (Rabinsky and Tarasova, 2009; Rabinsky and Tarasova, 2012; Tarasova, 2013), adopting a number of simplifying assumptions:

- the problem is considered in a one-dimensional axisymmetric formulation with a uniform distribution of the parameters at the boundaries of the circular adsorber;

- only one component of the gas stream – CO_2 is adsorbed;

- the heat release in the sorption layer is infinitesimal, and the flow and adsorbent temperatures are the same (the temperature of the layer is assumed to be a constant value). The assumption that the layer is isothermal makes it possible to reveal the influence of the determining parameters on mass transfer processes that are not complicated by thermal effects;

- the total pressure drop across the thickness of the granular adsorbent layer is absent (the hydraulic resistance of the fixed layer of granular sorbent is negligible);

- the mobile phase is incompressible and the CO_2 concentration in it is so small that it is possible to neglect the changes in the flux density due to the loss of adsorption (the physical characteristics of the initial gas mixture corresponding to the values for dry air).

In this case, the dynamics of the nonequilibrium isothermal adsorption (Montastruc *et al*., 2010) of carbon dioxide in a stationary grainy layer is described by the closed initial-boundary value task (Equation 1).

The first equation of system (Equation 1) is the equation of material balance, taking into account convection, longitudinal diffusion, and local mass flow. The second equation of system (Equation 1) describes the kinetics of sorption. The third equation of system (Equation 1) is the Langmuir adsorption isotherm. The last ratio of (Equation 1) includes the starting and the boundary conditions for the task. The initial conditions mean the absence of CO_2 in the layer, both in the free and bound states, which corresponds to the case of the complete desorption process. The boundary condition at $r = R_1$ corresponds to the task at the entrance to the layer of a certain concentration of carbon dioxide $\varphi_1(t)$. The boundary condition at $r = R_2$ means that there is no diffusion flux of CO_2 at the exit from the layer. Here $\rho(t,r)$ – mass concentration of CO_2 in air flowing through the layer with porosity ε; $a(t,r)$ – mass concentration of CO_2 absorbed per unit volume of sorbent; $\rho^*(t,r)$ – equilibrium value of CO_2 concentration in air, corresponding to the amount of absorbed substance $a(t,r)$ and determined by the adsorption isotherm; $a^*(t,r)$ – the concentration of absorbed CO_2 in the sorbent upon reaching the state of adsorption equilibrium; $u(r)$ is the velocity of air flow through the circular absorber; $D^*(r)$ – the effective coefficient of longitudinal diffusion of CO_2, taking into account the possible disruption of the piston structure of the flow in the granular layer; β – external diffusion kinetic coefficient; a_∞, B – constants of the Langmuir isotherm; t is the time; r is the radial coordinate.

RESULTS AND DISCUSSION:

3.1. Development of the algorithm for constructing the solution

The system (Equation 1) has no analytical solution. To construct a numerical solution, we used the *method of lines* (Formalev and Reviznikov, 2004; Formalev *et al*., 2018), which is a method of partial discretization of the task. This method involves approximating a part of the differential operators entering into equations using the finite difference relation, while the other part of the operators is stored in a differential form. In our case, the differential operators with respect to the spatial variable *r* entering the first equation of the system (Equation 1) were approximated by the ratio of central differences of the second order of accuracy, and all the differential operators with respect to time *t* preserved the longitudinal variant of the method of lines (Formalev and Reviznikov, 2004). It should be noted that the approximation of the boundary condition for $r = R_2$ by means of the ratio of finite differences on the left leads not only to the first order of accuracy of the entire initial-boundary value task with respect to the spatial variable, but also to the non-conservatively of the finite-difference scheme, since on the spatial steps adjacent to this boundary does not take into account the differential equation itself. I. e. at the boundary $r = R_2$, the conservation laws on the basis of which the system (Equation 1) is obtained are not observed in the finite-difference scheme.

To eliminate this phenomenon and preserve the order of approximation with respect to a spatial variable equal to two, in the finite-difference approximation of the boundary condition for $r = R_2$ we take into account the first and second equations of the system (Equation 1). To do this, we make the assumption that there exists on the given boundary a second-order derivative of the searched function $\rho(t,r)$ with respect to the variable *r*, and then expand on the exact solution the value of the grid function ρ_{N-1} in a neighborhood of the point $r = R_2$ in a Taylor series up to the third term inclusive, we obtain (Equation 1).

Substituting in (Equation 2) the value of the second derivative at the boundary node, obtained from the first and second equations of the system (Equation 1), we arrive at the expression for

determining the desired first derivative $\left.\frac{\partial\rho}{\partial r}\right|_N$ in the boundary node with the order $O\left(h^2\right)$.

As a result, we obtain the following Cauchy task for a normal non-homogeneous system of ordinary differential equations ($N + N$) -th order.

The evaluation of the characteristic times of the processes for the modeling conditions under consideration allows us to conclude that the system of ordinary differential equations (Equation 3) obtained is *rigid* (Shalashilin and Kuznetsov, 1999) in the sense that it corresponds to physical processes taking place with essentially different velocities. For the absorber under study, the characteristic time of the convection process is ~ 0.24 s; diffusion ~ 14.4 s, CO_2 absorption from the air flow ~ 0.1 s, saturation of the layer element at the concentration φ_1 – ~ 312.5 s (Rabinsky and Tarasova, 2012; Tarasova, 2013; Dantas *et al.*, 2011). It is known that the numerical integration of rigid systems by classical methods (for example, by explicit methods such as Adams or Runge-Kutta) entails enormous difficulties due to the existence of solution areas with essentially different behavioral patterns. This fact should be taken into account when developing the algorithm for calculating the system (Equation 3).

The most complete review of the current state of numerical methods for solving rigid systems of differential equations with extensive bibliography is presented in works (Shalashilin and Kuznetsov, 1999; Hayrer and Wanner, 1999; Butcher, 2008). One of the effective ways of constructing solutions to such problems is to use implicit multi-step methods based on the use of the *backward differentiation formula* (BDF) of the *k-th* order. A more general name for these methods is Gear's methods. The BDF methods are rigidly stable (in the sense of C.W. Gear (1971)) from $k = 1$ to $k = 6$ inclusive, therefore, to increase the integration of hard systems, an increase in the order of the formulas up to $k = 6$ is usually used. The search for the value of the integral function at the next step is usually carried out using the Newton-Raphson method. The rate of convergence of the iterative process imposes strong limitations on the magnitude of the integration step. At the same time, reducing the step (down to the minimum possible) does not always allow us to adapt to the local behavior of the solution and to reduce the amount of computation while observing the required accuracy. The optimal strategy for using BDF methods implies the existence of a procedure for automatically controlling the order of the formulas (with $k = 1$ to $k = 6$) and the step size. This requires calculating the estimate of the local error of the method and effective (in the sense of saving the computer's main memory) of computing, storing, and reproducing an array of previous decision values. In this work, we used the formulas of backward differentiation of variable order (up to $k = 5$ inclusive) with adaptive control of the magnitude of the integration step realized in the environment of computational mathematics MATLAB.

The authors of the work (Shalashilin and Kuznetsov, 1999) showed that the transformation of the Cauchy task for rigid systems of ordinary differential equations to the task of continuation of a solution with respect to the best parameter softens the rigidity of the original system, and, consequently, increases the efficiency of any numerical method for solving it. In this case, the best (in the sense of the computational aspect) parameter of the continuation of the solution is the length of the arc, computed along the curve, which is the solution. The transition to the best parameter is carried out with the help of an analytical λ-transformation that does not change the phase picture of the system and the integral curve of the task. The transformation improves the spectral characteristics of the system of equations under study-the eigenvalues and the width of the spectrum of the matrix of the system decrease.

After applying to the system (Equation 3) λ -transformation (Shalashilin and Kuznetsov, 1999) the task takes the form (Equation 4), where P_m is the right-hand sides of the corresponding equations of the system (Equation 3): when $m = \overline{1, N}$ – the right-hand sides of the equations for determining ρ_m, while $m = \overline{(N+1),(N+N)}$ – the right-hand sides of the equations for determining a_{m-N}.

The newly formulated Cauchy task (Equation 4) has several advantages over the Cauchy task (Equation 3). Thus, the right-hand sides of each equation (Equation 4) do not exceed one. This removes many problems associated with the unbounded growth of the right-hand sides of the system (Equation 3),

which allows us to integrate differential equations whose integral curves contain, for example, limit points whose derivatives go to infinity. Moreover, according to (Shalashilin and Kuznetsov, 1999), the quadratic error arising due to perturbation of the right-hand parts of the transformed system taking the smallest value. This is especially important in the numerical integration of the system (Equation 4) since the computational errors, in this case, will have the least effect on the solution.

Testing of the developed numerical algorithm is performed using a number of analytical solutions of model problems (Tikhonov and Samarskii, 1977; Sherwood *et al.*, 1982). The magnitude of the absolute error of the numerical solution, which determines the termination condition for the *m-th* iteration, was set by means of a special system variable *AbsTol*, whose values ranged from 10^{-6} to 10^{-8}. An estimate of the degree of accuracy of a numerical solution constructed using the developed algorithm was carried out by calculating its deviation from the corresponding analytical solution for each of the model problems considered. In all cases, a good agreement of the results was obtained. It is shown that the maximum absolute error of the calculations is of the same order with the *AbsTol* value.

3.2. Parametric calculations of adsorption

In order to study the nature of the course of the sorption of carbon dioxide with varying parameters of the process, a computational experiment was implemented, the plan of which was compiled taking into account the expert information and the results of full-scale tests on the model installation (Chou and Chen, 2004).

As a basic variant of calculating the process of adsorption of carbon dioxide, a variant with the following initial data was adopted (Tarasova, 2013; Tarasova, 2014; Tarasova *et al.*, 2015): mass flow of air through the circular absorber G = 815 m^3/h; concentration of CO_2 in the air at the entrance to the layer φ_1 = 0.3% by volume = $5.5 \cdot 10^{-3}$ kg/m^3; parameters of the Langmuir isotherm (at a layer temperature of 20 °C) for iron hydroxide B = 258 m^3/kg, a_∞ = 29.3 kg/m^3; external diffusion kinetic coefficient β = 10 s^{-1}.

The velocity of air flow through the circular absorber is determined from the continuity equation for an incompressible gas: $u(r) = \frac{u_{ent} \cdot R_1}{r}$, where u_{ent} – inlet velocity at the layer. The latter value is calculated from the total gas consumption G by the density ρ_{air} = 1.2 kg/m^3 flowing through the inner wall of the absorber with a cross-sectional area of F: $u_{ent} = \frac{G}{\rho_{air} \cdot F}$. Then, in accordance with the values indicated in Figure 1 size, we obtain: the radii of the cross-sections at the inlet and outlet R_1 = 0.11 m and R_2 = 0.23 m; $F = 2 \cdot \pi \cdot R_1 \cdot l$ = 0.453 m^2; u_{ent} = 0.5 m/s.

The effective coefficient of longitudinal diffusion of carbon dioxide through the sorbent layer is calculated by formula $D^*(r) = D \cdot \varepsilon^{1,2} + b \cdot u(r) \cdot d$ (Rachinsky, 1964), where D = $1{,}512 \cdot 10^{-5}$ m^2/s is the coefficient of molecular diffusion in the "air-CO_2" system, b is the dimensionless coefficient of the order of one, determined experimentally for stationary and nonstationary modes of matter transport in the granular layer. In the first approximation, we can assume that b = 1.

Numerical implementation of the developed algorithm and visualization of calculation results were carried out in the environment of computational mathematics MATLAB. The magnitude of the permissible absolute error of the solution was set equal to *AbsTol* = 10^{-8}. The number of points of the difference grid along the coordinate r was N = 500. The counting time of the variant with the specified input data on the workstation (processor – Intel (R) Core (TM) i3-3220 CPU @ 3.30 GHz, RAM – 16.0 GB) was ~ 17 s.

In Figure 2, *a* Figure 3, *a* is the space-time graphs of the change in the concentrations of CO_2 absorbed in the filtered gas $\rho(r - R_1, t)$ and absorbed CO_2 in the sorbent $a(r - R_1, t)$, and in Figure 2,*b*, Figure 3,*b* – the corresponding concentration profiles of free and absorbed carbon dioxide over the thickness of the adsorption layer at fixed times *t*. Figure 4 shows the output curve $\rho(t)$: time variation of CO_2 concentration in the air flow at the outlet from the layer ($r = R_2$). The graphs are plotted on a regular grid (at equidistant nodes). The transition from the adaptive step in time used in the internal calculations of the system (Equation 4) to the

uniform step was carried out by interpolating the system of solutions of the system (Equation 4) using the system functions of one-dimensional and two-dimensional tabular interpolation *interp1* and *interp2* (method – *spline* – cubic spline interpolation).

In a time equal to the gas-dynamic time $t = \tau_d = \int_{R_1}^{R_2} \frac{\varepsilon \cdot dr}{u(r)} = \varepsilon \cdot \frac{R_2^2 - R_1^2}{2 \cdot R_1 \cdot u_{ent}}$ ~ 0.15 s, the initial gap in the concentration levels (initial $\rho|_{t=0} = 0$ and input φ_1 = 5,5·10^{-3} kg/m^3 at $r = R_1$) is carried out together with the air flow out of the layer($r > R_2$). In this case, the formation of an initial profile of CO_2 concentration occurs (see Figure 2*b* for $t = \tau_d$). The amount of CO_2 absorbed in such a short time is very small – on the scale of Figures 3,*b* $a(r - R_1, \tau_d) = 0$. Further ($t > \tau_d$), the front begins to move slowly along the line as the sorbent layers are sequentially saturated. The velocity of the profile movement is determined by the amount of material supplied to the layer per unit of time ($\varphi_1 \cdot u(r)$) and practically does not depend on the kinetics of sorption and porosity of the layer, which plays an important role only in the process of formation of the frontline. For each fixed cross-section, the frontline propagation along the layer means a monotonic increase in the concentration of CO_2 in the air to the level of the inlet concentration φ_1. The amount of absorbed substance is increased accordingly to the equilibrium concentration $a^*(\varphi_1)$, determined by the sorption isotherm (the third equation of system (Equation 1)). In this basic version, the capacity of the layer a^* = 17.2 kg/m^3 (Figure 3). Beginning at some point in time, the substance passes through the layer, after which the concentration of CO_2 at the outlet from the layer increases monotonically and asymptotically tends to the level of the inlet concentration $\rho = \varphi_1$ (Figure 4). With the parameters of the basic variant, the full saturation of the burden layer proceeds for a time t ~ 2000 s.

Subsequent parametric calculations were performed by varying the following values (Tarasova, 2014; Tarasova *et al.*, 2015): the gas concentration at the entrance to the absorber layer φ_1, the gas filtration rate at the u_{ent} inlet, the kinetic adsorption coefficient β. When one of the values was changed, the others were assumed to be equal to the corresponding values of the base variant.

In Figure 5,*a*, Figure 6, *a* there are spatial graphs of the concentrations of free $\rho(r - R_1, \varphi_1)$ and related $a(r - R_1, \varphi_1)$ carbon dioxide over the thickness of the adsorption layer at a time t = 1000 s with a change in the value of the inlet concentration φ_1, and in Figure 5,*b*, Figure 6,*b* – the corresponding concentration profiles of free and absorbed CO_2 at time t = 500 s and 1000 s at the values of the inlet concentration φ_1 = (3.6, 5.5, 9.0)·10^{-3} kg/m^3. In Figure 7 shows the output region (Figure 7a) and curves (Figure 7b) of free CO_2 concentrations in air for the same input concentration values φ_1, as in Figure 5, 6.

As expected, as the input concentration increases, the saturation time of the layer decreases, which is due to an increase in the current density of the substance $\varphi_1 \cdot u(r)$, which is brought to the sorbent layer. This is reflected in a more rapid advancement of profile concentrations of the rim $\rho(t, r)$ and absorbed $a(t, r)$ carbon dioxide (Figure 5, 6) and an increase in the steepness of the output curves (Figure 7).

Figures 8-10 shows similar surface and curves for different values of the gas filtration rate at the inlet of the absorber layer u_{ent} = 0.25; 0.5, and 1 m/s. In general, the velocity increase leads to the same effects as the growth of the inlet concentration, which is also explained by the increase in the current density $\varphi_1 \cdot u(r)$. However, in this case, there is a fundamental difference: the fixed thickness from a certain level of speed, there is a so-called "cumulative slip" when the velocity of the gas flow is so high that the substance has no time to absorb and passes through the layer of unsaturated sorbent (Shafeeyan *et absal.*, 2014). The output curves (Figure 10) start almost immediately from a certain final concentration value. With the parameters considered in this work, the breakthrough is observed starting with u_{ent} = 0.5 m/s.

Calculated surfaces and concentration

profiles for different values of the kinetic coefficient β = 5, 10, and 20 s^{-1} are shown in Figures 11-13. With the growth of β the steepness of the profiles and, correspondingly, the output curves increases (Figure 13). For a fixed layer thickness, the small values of the coefficient β lead to a bypass in the concentration already at $t = \tau_d$, as in the case of sufficiently high values of the flow velocity.

To verify the adequacy and assess the degree of reliability of the developed mathematical model and the algorithm for constructing a numerical solution, verification and validation procedures were used. Unfortunately, the limited volume of the article does not allow us to discuss this part of the research in the proper way. The results of the calculations were compared with the experimental data on the sorption of carbon dioxide in the absorber of the model installation for atmospheric regeneration. A good qualitative and quantitative agreement of the results was obtained (the maximum relative error of the computational experiment did not exceed 12% for the operating ranges of the change in the input parameters). Small discrepancies consisted of a more gradual increase in the calculated values of CO_2 concentrations in the air flow at the exit from the absorber in comparison with the experimentally measured values. In all probability, this is due to the somewhat larger value of the sorption capacity, which is embedded in the mathematical model through the Langmuir sorption isotherm, than the actual capacitance value (available in the experiment). The second reason for these discrepancies may be the mathematical model itself, which does not take into account at this stage the thermal effects and features of the distribution of material flow in the near-wall zones of the absorber.

CONCLUSIONS:

1. An adequate mathematical model is proposed for the dynamics of nonequilibrium isothermal adsorption of carbon dioxide during the filtration of an incompressible gas mixture through a fixed axisymmetric sorbent layer.

2. An algorithm for constructing a numerical solution of the problem using the longitudinal variant of the method of straight lines, the method of continuation of the solution with respect to the best parameter, and implicit multi-step formulas for differentiating backwards with adaptive control of the order of the formulas and the magnitude of the integration step are developed.

3. Parametric calculations of the adsorption of carbon dioxide by sorbent based on iron hydroxide in a wide range of determining parameters: the inlet gas concentration, the gas filtration rate, and the kinetic adsorption coefficient.

4. Verification and validation of the developed software were performed by comparing the calculated and experimental data obtained in the model installation. It is shown that the computational experiment fairly correctly reproduces the main features of the process of isothermal adsorption.

ACKNOWLEDGEMENTS

The work was supported by the Russian Foundation for Basic Research (project code 17-08-01527-a).

REFERENCES:

1. Besedova, E., Bobok, D., Bafrncova, S., Steltenpohl, P. *Chemical Papers*, **2004**, *58(6),* 391-396.
2. Budiman, H., Zuas, O. *Periódico Tchê Química*, **2015**, *12(24)*, 7-17.
3. Butcher, J.C. *Numerical methods for ordinary differential equations*, Chichester: John Wiley & Sons Ltd, **2008**.
4. Chou, C.T., Chen, C.Y. *Separation and Purification Technology*, **2004**, *39*, 51-65.
5. Dantas, T.L.P., Luna, F.M.T., Silva Jr., I.J., Torres, A.E.B., de Azevedo, D.C.S., Rodrigues, A.E., Moreira, R.F.P.M. *Brazilian Journal of Chemical Engineering*, **2011**, *28(3)*, 533-544.
6. Formalev, V.F., Kolesnik, S.A., Kuznetsova, E.L. *Composites: Mechanics, Computations, Applications*, **2018**, *9(3)*, 223-237.
7. Formalev, V.F., Kolesnik, S.A., Kuznetsova, E.L. *High Temperature*, **2015**, *53(5)*, 697-702.
8. Formalev, V.F., Reviznikov, D.L. *Numerical methods*, Moscow: FIZMATLIT, **2004**.
9. Gear, C.W. *Numerical initial value problems in ordinary differential equations*, New Jersey: Prentice-Hall Inc., **1971**.
10. GOST R 50804-95. *The habitat of an astronaut in a manned spacecraft. General medical and*

technical requirements, Moscow: IPK Publishing house of standards, **1995**.

11. Hayrer E., Wanner G. *Solution of ordinary differential equations. Hard and differential-algebraic problems*, Moscow: Mir, **1999**.
12. Keltsev, N.V. *Basics of adsorption technique*, Moscow: Khimiya, **1984**.
13. Kuznetsova, E.L., Tarasova, A.N. Mathematical modeling of heat and mass exchange processes in the adsorbers of the pre-drying unit of the air purification system, *Materials of the XIV International Symposium "Dynamic and Technological Problems of Mechanics of Constructions and Continuous Media" named after A.G. Gorshkov*, Moscow: "ID MEDPRAKTIKA-M", **2008**.
14. Li, Sh., Deng, Sh., Zhao, L., Zhao, R., He, J., Sun, T. *Energy Procedia*, **2017**, *142*, 3244-3251.
15. Montastruc, L., Floquet, P., Mayer, V., Nikov, I., Domenech, S. *Chinese Journal of Chemical Engineering*, **2010**, *18(4)*, 544-553.
16. Posternak, N.V., Putin, S.B., Simanenkov, S.I., Gatapova, N.T. *Bulletin of TSTU*, **2012**, *18(1)*, 173-181.
17. Rabinsky, L.N., Tarasova, A.N. Experimental determination of the main characteristics of the adsorption layer of the atmosphere purification system, *Materials XVII International Symposium "Dynamic and technological problems of mechanics of structures and continuous media" named after A.G. Gorshkov*, Moscow: TR-print LLC, **2011**.
18. Rabinsky, L.N., Tarasova, A.N. Formation of physical factors, initial and boundary conditions in the construction of a mathematical model of sorption systems, *Materials of the XVIII International Symposium "Dynamic and Technological Problems of Mechanics of Constructions and Continuous Media" named after A.G. Gorshkov*, Moscow: TR-print LLC, **2012**.
19. Rabinsky, L.N., Tarasova, A.N. Investigation of physical processes in the adsorption layer using numerical simulation, *Materials of the II All-Russian scientific-practical student's school-seminar "Computer engineering in industry and universities", dedicated to the 80th anniversary of the MAI,* Moscow: MAI-PRINT, **2009**.
20. Rachinsky, V.V. *Introduction to the general theory of sorption dynamics and chromatography*, Moscow: Nauka, **1964**.
21. Shafeeyan, M.S., Daud, W.M.A.W., Shamiri, A. *Chemical Engineering Research and Design*, **2014**, *92*, 961-988.
22. Shalashilin, V.I., Kuznetsov, E.B. *The method of continuation of the solution with respect to the parameter and the best parametrization*, Moscow: Editorial URSS, **1999**.
23. Sherwood, T., Pigford, R., Wilkie, C. *Mass transfer*, Moscow: Khimiya, **1982**.
24. Shumyatsky, Yu.I. *Industrial adsorption processes*, Moscow: KolosS, **2009**.
25. Tarasova, A.N. Modeling of mass transfer processes in a stationary isothermal adsorption layer, *Materials of the XIX International Symposium "Dynamic and Technological Problems of Mechanics of Constructions and Continuous Media" named after A.G. Gorshkov*, Moscow: TR-print LLC, **2013**.
26. Tarasova, A.N. *Nonlinear World*, **2011**, *9(7)*, 403-410.
27. Tarasova, A.N. Parametric calculations of mass transfer processes in a stationary isothermal adsorption layer, *Materials of the XX International Symposium "Dynamic and Technological Problems of Mechanics of Constructions and Continuous Media" named after A.G. Gorshkov,* Moscow: TR-Print LLC, **2014**.
28. Tarasova, A.N., Kurbatov, A.S., Astapov, A.N. *Nonlinear World*, **2015**, *13(1)*, 31-44.
29. Tarasova, A.N., Rabinsky, L.N. Investigation of the thermal state of the adsorbent in the regenerating unit for air purification, *Materials of the All-Russian Scientific and Technical Conference "New Materials and Technologies – NMT-2010"*, Moscow: MATI Publishing and Printing Center, **2010**.
30. Tikhonov, A.N., Samarskii, A.A. *Equations of mathematical physics*, Moscow: Nauka, **1977**.

$$\begin{cases} \varepsilon \cdot \dfrac{\partial \rho(t,r)}{\partial t} + u(r) \cdot \dfrac{\partial \rho(t,r)}{\partial r} = D^*(r) \cdot \dfrac{\partial^2 \rho(t,r)}{\partial r^2} - \dfrac{\partial a(t,r)}{\partial t}; \\ \dfrac{\partial a(t,r)}{\partial t} = \beta \cdot \left[\rho(t,r) - \rho^*(t,r) \right]; \\ a^*(t,r) = \dfrac{a_\infty \cdot B \cdot \rho(t,r)}{1 + B \cdot \rho(t,r)}; \\ t = 0: \quad \rho(t,r)\big|_{t=0} = 0, \quad a(t,r)\big|_{t=0} = 0; \\ r = R_1: \quad \rho(t,r)\big|_{r=R_1} = \varphi_1(t); \quad r = R_2: \quad \left.\dfrac{\partial \rho(t,r)}{\partial r}\right|_{r=R_2} = 0. \end{cases} \tag{1}$$

$$\rho_{N-1} = \rho_N - \left.\frac{\partial \rho}{\partial r}\right|_N \cdot h + \left.\frac{\partial^2 \rho}{\partial r^2}\right|_N \cdot \frac{h^2}{2} + O\left(h^3\right). \tag{2}$$

$$\begin{cases} \dfrac{d\rho_1}{dt} = \dfrac{1}{\varepsilon} \cdot \left[u_1 \cdot \dfrac{\varphi_1(t) - \rho_2}{2 \cdot h} + D_1^* \cdot \dfrac{\rho_2 - 2 \cdot \rho_1 + \varphi_1(t)}{h^2} + \beta \cdot \left(\rho_1^* - \rho_1 \right) \right]; \\ \dfrac{d\rho_i}{dt} = \dfrac{1}{\varepsilon} \cdot \left[u_i \cdot \dfrac{\rho_{i-1} - \rho_{i+1}}{2 \cdot h} + D_i^* \cdot \dfrac{\rho_{i+1} - 2 \cdot \rho_i + \rho_{i-1}}{h^2} + \beta \cdot \left(\rho_i^* - \rho_i \right) \right], \quad i = \overline{2,(N-1)}; \\ \dfrac{d\rho_N}{dt} = \dfrac{1}{\varepsilon} \cdot \left[2 \cdot D_N^* \cdot \dfrac{\rho_{N-1} - \rho_N}{h^2} + \beta \cdot \left(\rho_N^* - \rho_N \right) \right]; \\ \rho_j\big|_{t=0} = \rho(0, r_j) = 0, \quad r_j = R_1 + (j-1) \cdot h, \quad h = \dfrac{R_2 - R_1}{N-1}, \quad j = \overline{1,N}; \\ \dfrac{da_j}{dt} = \beta \cdot \left(\rho_j - \rho_j^* \right); \quad a_j\big|_{t=0} = a(0, r_j) = 0. \end{cases} \tag{3}$$

$$\begin{cases} \dfrac{dq_m}{d\lambda} = \dfrac{P_m}{Q}; \quad \dfrac{dt}{d\lambda} = \dfrac{1}{Q}; \quad q_m(0) = 0; \quad t(0) = 0; \quad m = \overline{1,(N+N)}; \\ Q = \sqrt{1 + \sum\limits_{m=1}^{N+N} \left(P_m \right)^2}; \quad q_m = \begin{cases} \rho_m, \text{ если } m = \overline{1,N}; \\ a_{m-N}, \text{ если } m = \overline{(N+1),(N+N)}, \end{cases} \end{cases} \tag{4}$$

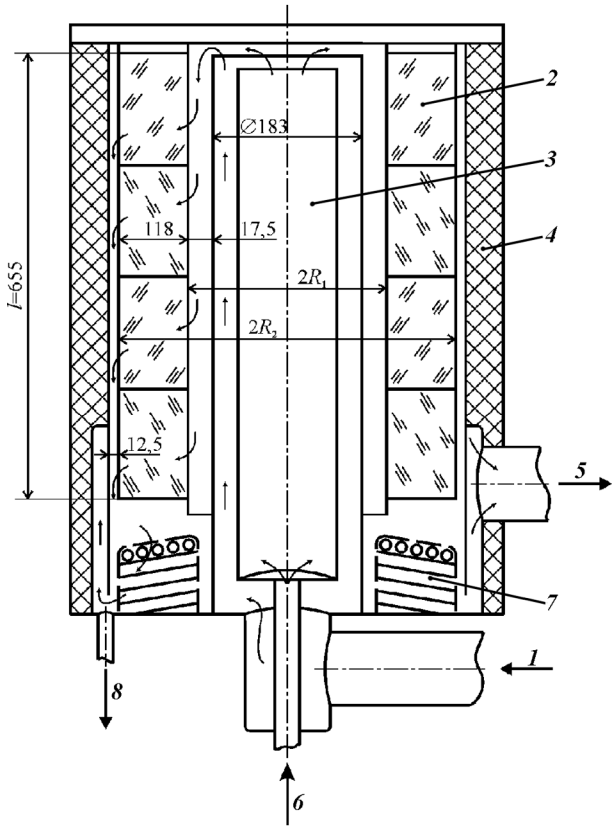

Figure 1. *The absorber of the carbon dioxide absorption unit:*
1 *– air inlet;* ***2*** *– sorbent;* ***3*** *– steam generator;* ***4*** *– thermal insulation;*
5 *– air outlet;* ***6*** *– water;* ***7*** *– condenser;* ***8*** *– condensate*

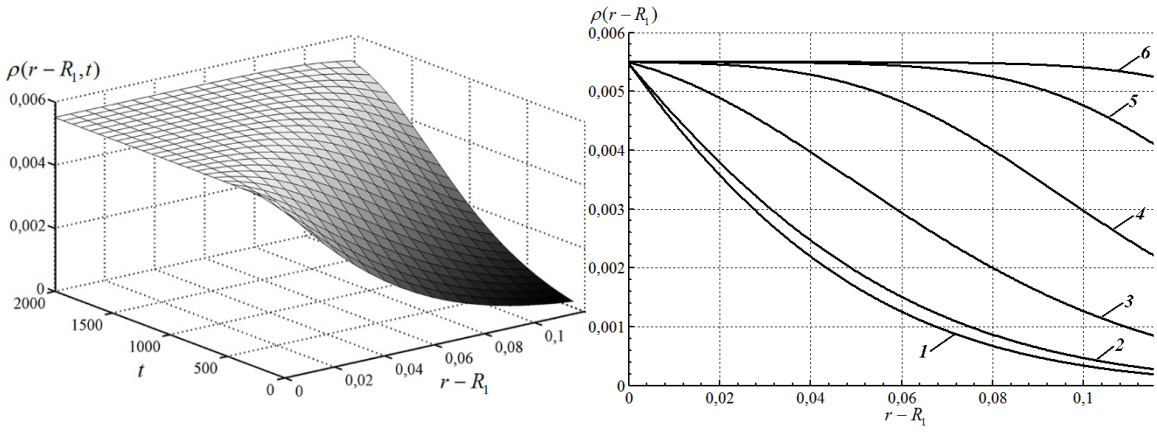

a) *b)*

Figure 2. *Areas (a) and profiles (b) of free CO_2 concentrations in the filtering gas along the thickness of the adsorption layer at time t:*
1 *– τ_d = 0.15 s;* ***2*** *– 100 s;* ***3*** *– 500 s;* ***4*** *– 1000 s;* ***5*** *– 1500 s;* ***6*** *– 2000 s*

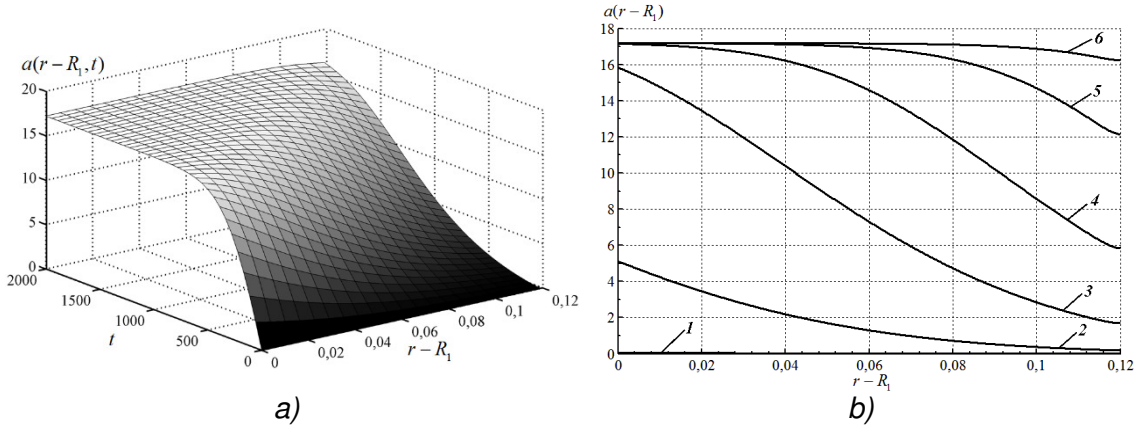

a) b)

Figure 3. *Areas (a) and profiles (b) concentrations of absorbed CO_2 in the sorbent along the thickness of the adsorption layer at time t:*
1 *– τ_d = 0.15 s;* ***2*** *– 100 s;* ***3*** *– 500 s;* ***4*** *– 1000 s;* ***5*** *– 1500 s;* ***6*** *– 2000 s*

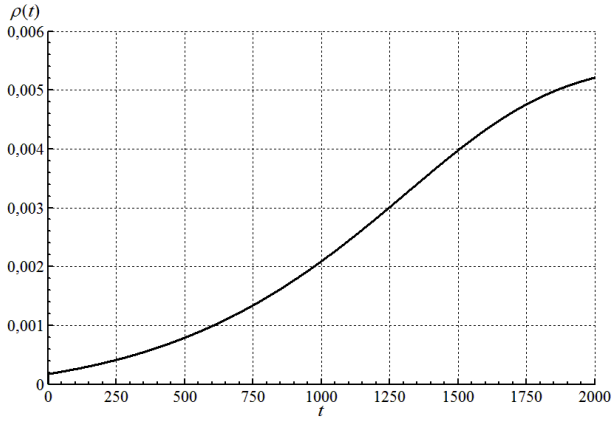

Figure 4. *The change in CO_2 concentration in the air flow at the outlet from the adsorption layer*

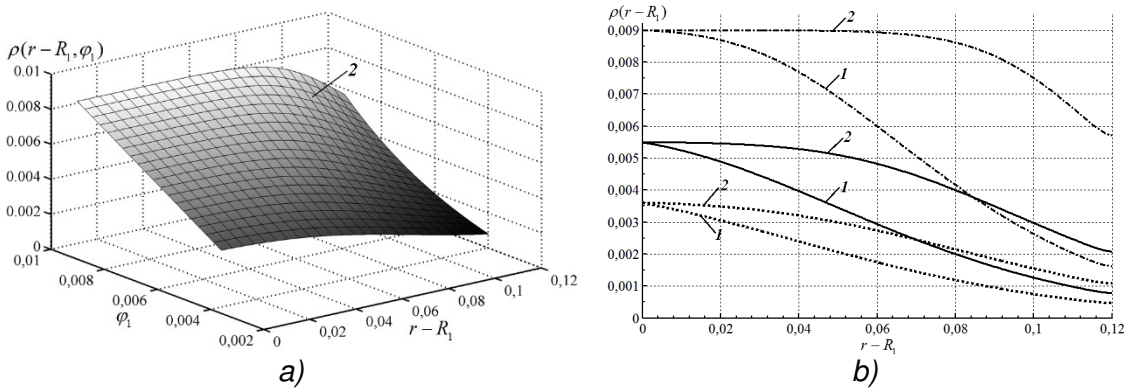

a) b)

Figure 5. *Areas (a) and profiles (b) of free CO_2 concentrations in the filtered gas along the thickness of the adsorption layer at different concentrations φ_1 at the entrance to the absorber layer at time t:* ***1*** *– 500 s;* ***2*** *– 1000 s; ····· φ_1 = 3.6·10^{-3} kg/m^3, ——— φ_1 = 5.5·10^{-3} kg/m^3, –·–·– φ_1 = 9.0·10^{-3} kg/m^3*

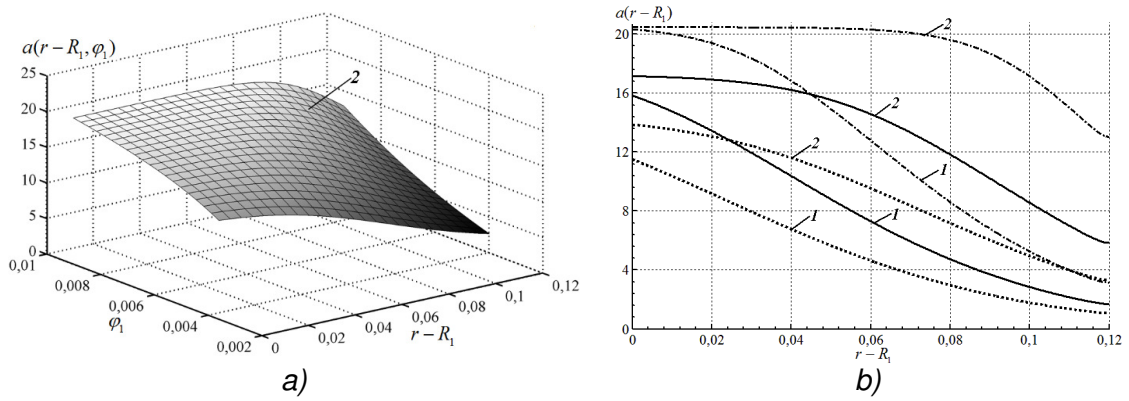

Figure 6. *The regions (a) and profiles (b) of the absorbed CO_2 concentrations in the sorbent along the thickness of the adsorption layer at different concentrations φ_1 at the entrance to the layer absorber at time t:* ***1*** *– 500 s;* ***2*** *– 1000 s; ····· φ_1 = 3.6·10^{-3} kg/m^3, ——— φ_1 = 5.5·10^{-3} kg/m^3, —·—·— φ_1 = 9.0·10^{-3} kg/m^3*

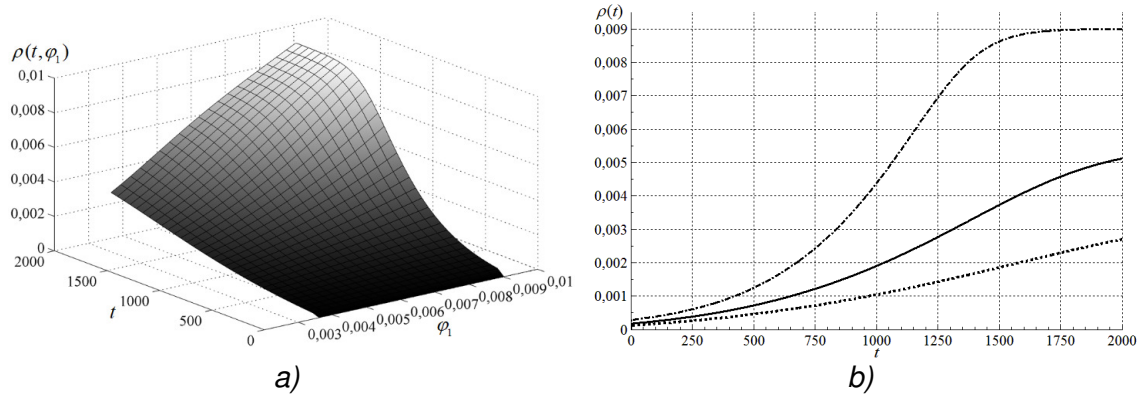

Figure 7. *Areas (a) and curves (b) of CO_2 concentrations in the air flow at the outlet from the adsorption layer at different concentrations at the inlet to the absorber layer: ····· φ_1 = 3.6·10^{-3} kg/m^3, ——— φ_1 = 5.5·10^{-3} kg/m^3, —·—·— φ_1 = 9.0·10^{-3} kg/m^3*

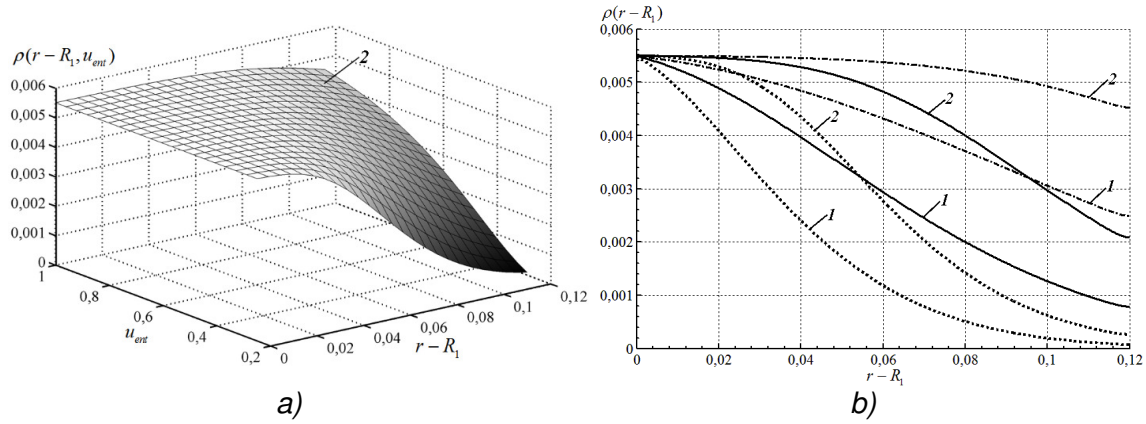

Figure 8. *Areas (a) and profiles (b) of free CO_2 concentrations in the filtered gas along the thickness of the adsorption layer at different air velocities at the entrance to the absorber layer at time t:* ***1*** *– 500 s;* ***2*** *– 1000 s; ····· u_{ent} = 0.25 m/s, ——— u_{ent} = 0.5 m/s, —·—·— u_{ent} = 1 m/s*

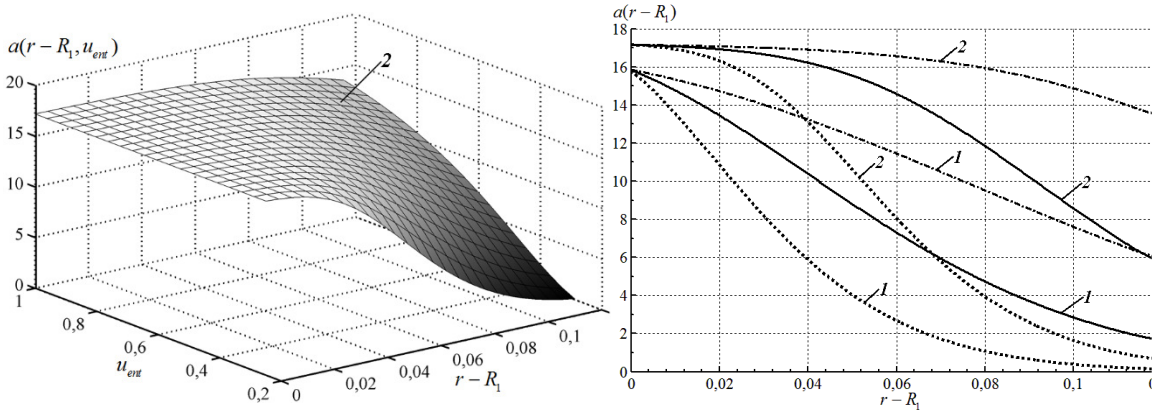

Figure 9. *Areas (a) and profiles (b) of absorbed CO_2 concentrations in the sorbent along the thickness of the adsorption layer at different air velocities at the inlet to the absorber layer at time t:* ***1*** *– 500 s;* ***2*** *– 1000 s; ····· u_{ent} = 0.25 m/s, ——— u_{ent} = 0.5 m/s, –·–·– u_{ent} = 1 m/s*

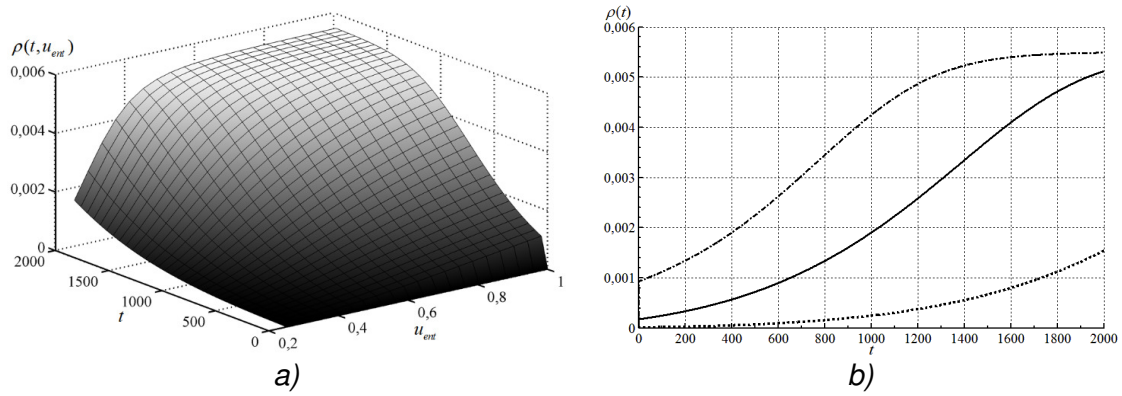

Figure 10. *Areas (a) and curves (b) of CO_2 concentrations in the air flow at the outlet from the adsorption layer at different air velocities at the entrance to the absorber layer: ····· u_{ent} = 0.25 m/s, ——— u_{ent} = 0.5 m/s, –·–·– u_{ent} = 1 m/s*

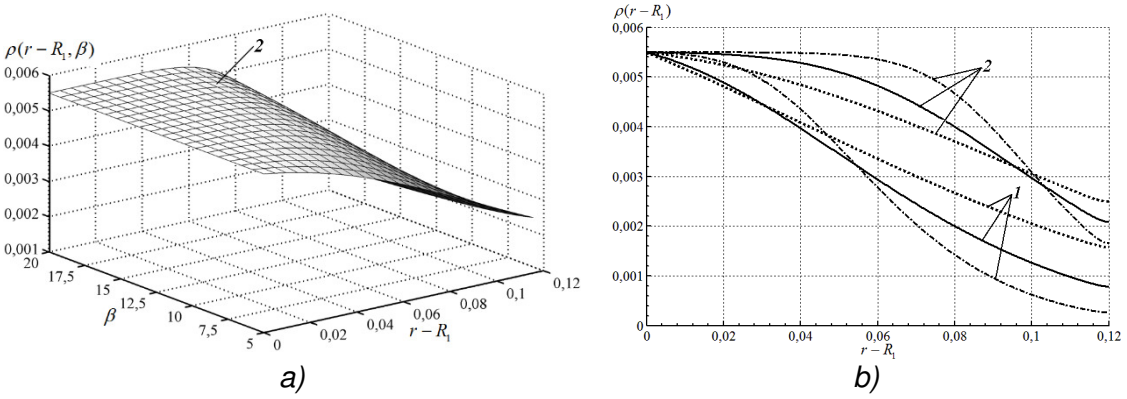

Figure 11. *Areas (a) and profiles (b) of free CO_2 concentrations in the filtered gas along the thickness of the adsorption layer at different values of the kinetic coefficient at time t:* ***1*** *– 500 s;* ***2*** *– 1000 s; ····· β = 5 s^{-1}, ——— β = 10 s^{-1}, –·–·– β = 20 s^{-1}*

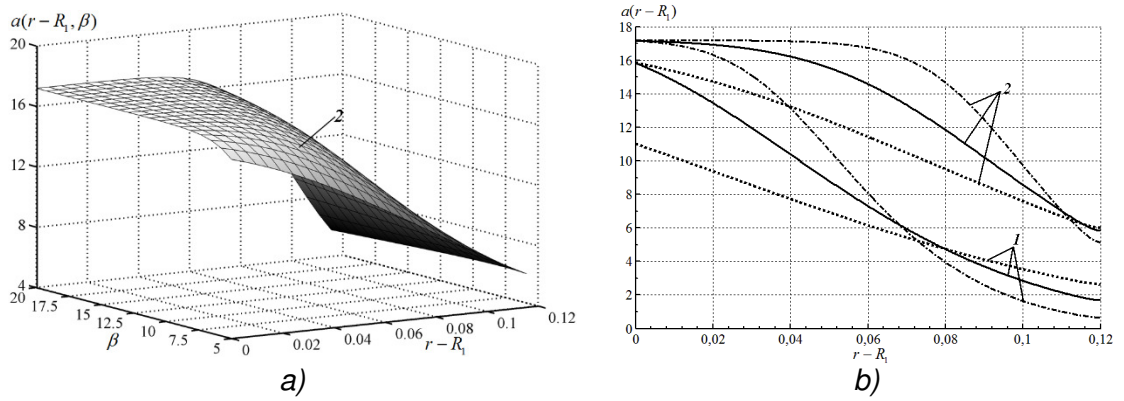

Figure 12. *Areas (a) and profiles (b) of the absorbed CO_2 concentrations in the sorbent along the thickness of the adsorption layer at different values of the kinetic coefficient at time t:* ***1*** *– 500 s;* ***2*** *– 1000 s; ····· β = 5 s^{-1}, ——— β = 10 s^{-1}, –·–·– β = 20 s^{-1}*

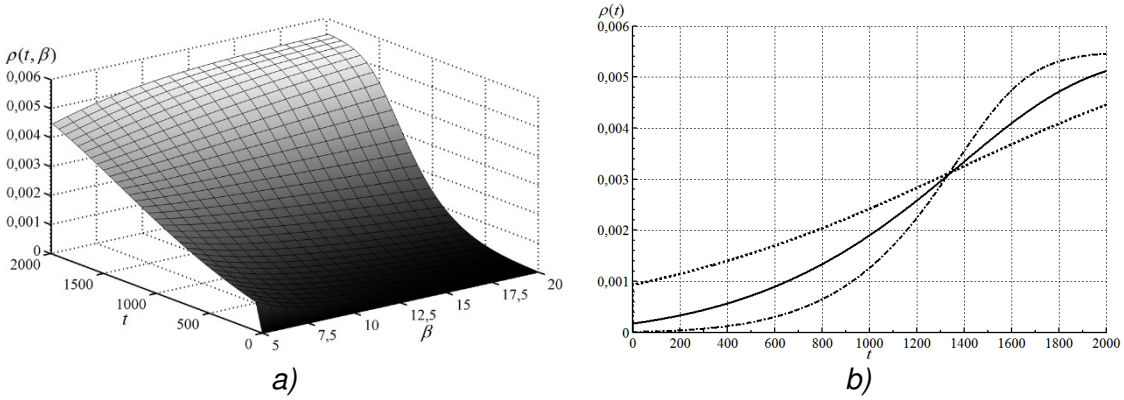

Figure 13. *Areas (a) and curves (b) of CO_2 concentrations in the air flow at the outlet from the adsorption layer at different values of the kinetic coefficient: ····· β = 5 s^{-1}, ——— β = 10 s^{-1}, –·–·– β = 20 s^{-1}*